Design and Development of a Rectifier Stage Topology for µgrid

M.Manigandan, Dr.B.Basavaraja and G.Srikanth

Abstract— Microgrids (µ-grids) are new way of electrical systems consisting of distributed energy sources and sensitive loads. The subjective of operation is to distribute stable and quality electric power. As it is intricate for the use of a real µ-grid for laboratory project, development of a model that can be connected and utilized for nominal loads. The design and development of a new system configuration of the front-end rectifier stage for µ-grid is presented in this paper. First, the mathematical model of µ-grid is developed and this configuration allows the µ-grid to supply the load separately or simultaneously depending on the availability of the energy sources. Proposed hardware implementation involves Cuk-SEPIC fused converter, a cascaded multilevel inverter and a variable load. The inherent nature of this Cuk-SEPIC fused converter, additional input filters are not necessary to filter out high frequency harmonics. For extraction of maximum power from the Solar PV and wind an adaptive MPPT is used specifically a standard perturb and observe method is used for Solar PV Hardware and Simulation results will given the scope for the use of proposed Rectifier Stage Topology.

Index Terms— Microgrid (µ-grid), Cuk converter, SEPIC converter, MLCI

———————————— ◆ ————————————

1 INTRODUCTION

The electrical grid is tending to be more distributed, intelligent, and flexible. The trend of this new grid is to become more and more distributed, and hence the energy generation and consumption areas cannot be conceived separately. Nowadays electrical and energy engineering have to face a new scenario in which small distributed power generators and dispersed energy storage devices have to be integrate together into the grid. A trend for the change in the performance of existing distributed generations from backup to immediate energy supply and to have a malleable contact approach which sets up for the concept of Microgrid have become incipient. Microgrids (µ-grids) have becoming an important concept to integrating distributed renewable sources and energy storage systems.

Managerial and technology, variation for power generation, environmental and economical enticements and the expansion of smaller generating systems like solar, wind, microturbine power generators have opened new goal for on-site power generation by electricity consumers [1-4]. Among all sources of µ-grid Solar PV and Wind energy holds the most potential to meet our demands. Specifically Wind energy has a high potential in supplying large amount of power but it depends on the velocity of wind at particular location. Similarly, Solar PV is also having high potential in severing load but it mostly serves potentially in the day light. By considering the drawbacks and their inherent natures a common maximum power point tracking (MPPT) algorithms is made for coupled source for improving the output power, power transfer efficiency and reliability significantly

When an individual input source is insufficient in convention the local load demands, the alternate energy source can satisfy for the change.

Many scholars have been suggested a simpler multi-input structure by integrating renewable sources from the DC-end with MPPT for each renewable source and many have proposed a fusion of the buck and buck-boost converter and given a scope for further development [5-7]. With the literature a passive input filters are required to remove passive input

remove the hike in current harmonics frequencies squeeze into generators of wind turbine [8-9]. The increase in power loss and decrease in lifespan of generators can be reduced by reducing harmonic content in generator.

In this paper, an alternative multi-input rectifier topology is proposed for µ-grid (hybrid Solar/Wind system). Hardware design is a blend of the Cuk and SEPIC converters [10-12]. The proposed topology will give a scope for the use of µ-grid with MPPT for individual source and rectification circuits. Hardware and Simulation results are lend to check with the utility of the proposed system.
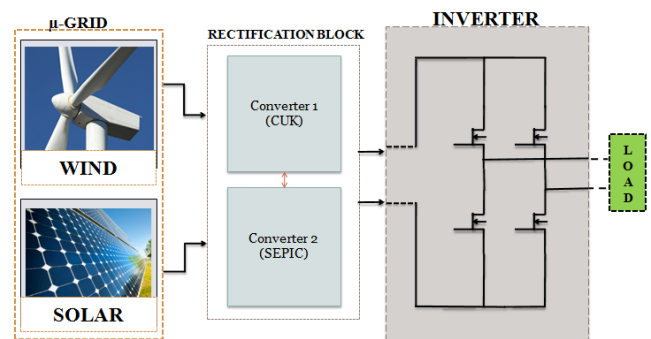

Fig.1: Hybrid system with multi-connected boost converter

2 MICROGRID (µ-GRID)

2.1 Solar PV:

Photo Voltaic module basically in build with solar cell and it is the element in charge of transforming the sun rays or photons directly into power. For a Solar system, the voltage output is a constant DC whose magnitude depends on the composition in which the solar cells/ modules are connected [14]. The process of regulating the voltage and current output of the array must be upgraded based on the weather conditions such as irradiation.

Figure 2 & 3 represents the simulation results of solar with and without MPPT and I-V and P-V characteristics using

Guide. Maximum power point tracking (MPPT) algorithm is developed to constantly extract the maximum amount of power from the array under varying conditions. The Ideal equations determining the I-V characteristics of the PV cell is.

$$I = I_{il} - I_{diode} \qquad (1)$$

Where $I_{diode} = I_{LCdiode} * \left| \exp\left(\frac{qv}{a_d \cdot kT}\right) - 1 \right|$

$$I = I_{il} - I_{LCdiode} * \left| \exp\left(\frac{qv}{a_d \cdot kT}\right) - 1 \right| \qquad (2)$$

Where, I_{il} is the current generated by the sun irradiation, I_{diode} is the diode equation, $I_{LCdiode}$ cell is the leakage current of the diode.
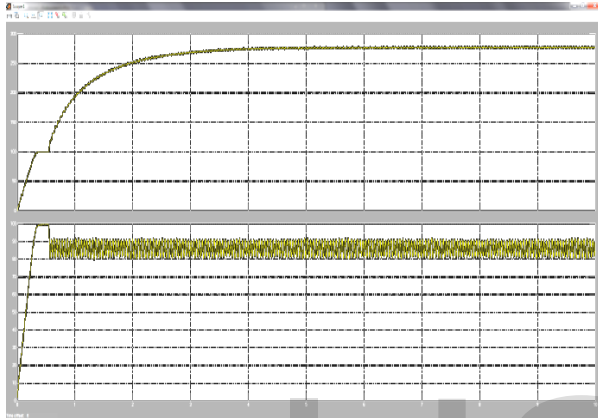

Fig.2: Simulation Output of Solar with and without MPPT

Electron charge q = 1.60217646*10-19 C, k is the Boltzmann constant and T is the temperature, and 'a_d' is the diode ideally constant.
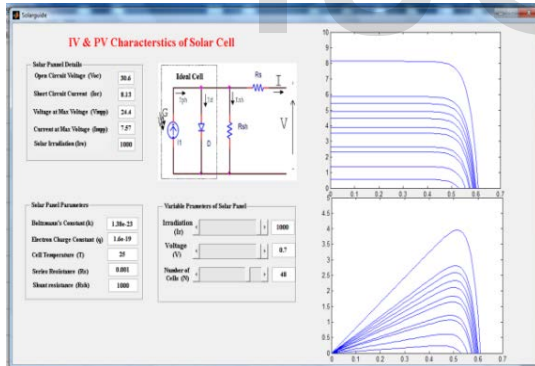

Fig.3: I-V, P-V characterstics using Guide

2.2 Wind:

he main components of a wind energy conversion system, including turbine blade, a gearbox, Converters, Inverters, Control circuits etc along with cables, filters, ground support equipment and interconnection equipment [13,15]. Wind turbine captures power from wind by means of turbine blades and converts it into mechanical power and Fig.2 represents the simulation output of Wind. The power contained in the wind is given by the kinetic energy of the flowing air mass per unit time as follows

$$P_w = \frac{1}{2}(Mass\ of\ air\ per\ unit\ time) * (Wind\ velocity)^2$$
$$= \frac{1}{2} * \rho * A_r * V_w{}^3 \qquad (3)$$

Where P_w : Power contained in wind (in watts),
         ρ : Air density,

A_r : Rotor area in (square meter)
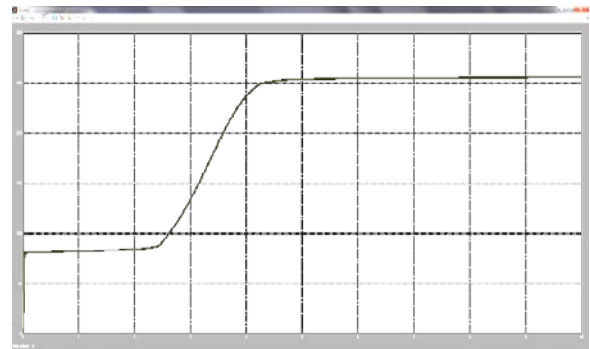V_w : Wind velocity without rotor interference,

Fig.4: Simulation Output of Wind

3   PROPOSED RECIFIER STAGE TOPOLOGY

The Power electronics research community and industry have reacted to this demand in two different ways: developing semiconductor technology to reach higher nominal voltages and currents. A system diagram of the proposed rectifier stage of a hybrid energy system is shown in Figure 5, The fusion of the two converters is achieved by reconfiguring the two existing diodes from each converter and the shared utilization of the Cuk output inductor by the SEPIC converter. This configuration allows each converter to operate normally individually in the event that one source is unavailable. Figure5 illustrates the case when only the wind source is available. In this case, D_1 turns off and D_2 turns on; the proposed circuit becomes a SEPIC converter and the input to output voltage relationship is given by (4). On the other hand, if only the PV source is available, then D_2 turns off and D_1 will always be on and the circuit becomes a Cuk converter as shown in Figure 6.The input to output voltage relationship is given by (5). In both cases, both converters have step-up/down capability, which provide more design flexibility in the system if duty ratio control is utilized to perform MPPT control.

$$\frac{V_{dc}}{v_1} = \frac{d_2}{a_d} \qquad (4)$$

$$\frac{V_{dc}}{v_1} = \frac{d_1}{a_d} \qquad (5)$$

The mathematical expression that relates the total output voltage and the two input sources are been illustrated

To find an expression for the output DC bus voltage, V_{dc}, the volt-balance of the output inductor, according to Figure 8. It is observed that V_{dc} is simply the sum of the two output voltages of the Cuk and SEPIC converter. This further implies that V_{dc} can be controlled by d_1 and d_2 individually or simultaneously

Table1:Modes of switching states

M_1, M_2	On-On $0<t<d_1T_s$	On-off $d_1T_s<t<d_2T_s$	Off-Off $d_2T_s<t<T_s$
i_1	$i_{L1=I_{ipv}} + \frac{pv}{r}t$	$i_{I1} = I_{i,pv} + \left[\frac{pv}{r}\right]$	$i_{I1} = I_{i,pv} + \left[\frac{pv}{r} - \frac{c1}{r}\right]$
i_2	$i_{I2} = I_{dc} + \left[\frac{c1}{r}\right]$	$i_{I2} = I_{dc} + \left[\frac{c1}{r}\right]t$	$i_{I2} = I_{dc} - \left[\frac{dc}{r}\right]t$
i_3	$i_{I3} = I_{i,w} + \left[\frac{w}{r}\right]t$	$i_{I3} = I_{i,w} + \left[\frac{w}{r}\right]t$	$i_{I3} = I_{i,w} + \left[\frac{w}{r} - \frac{c2}{r}\right]$

Figure 5: Proposed rectifier stage for a Hybrid wind/PV system

respective duty cycle ($d1$)

$$V_{dc} = \left\{\frac{u_1}{u_1'}\right\}v_{c1} + \left(\frac{u_2}{u_2'}\right)v_{c2} \qquad (6)$$
$$V_{dc} = \left\{\frac{u_1}{\cdot}\right\}V_{PV} + \left(\frac{u_2}{\cdot}\right)V_W \qquad (7)$$

Therefore by adjusting the respective duty cycles for each energy source, maximum power point tracking can be achieved.

$$v_{ds1} = V_{PV}\left(1 + \frac{u_1}{\cdot}\right) \qquad (8)$$
$$v_{ds2} = V_W\left(1 + \frac{d_2}{\cdot}\right) \qquad (9)$$

$$i_{ds1,pk} = I_{i,PV} + I_{dc,avg} + \frac{pv \cdot u_1 \cdot s}{2l}$$

Circuit Integration

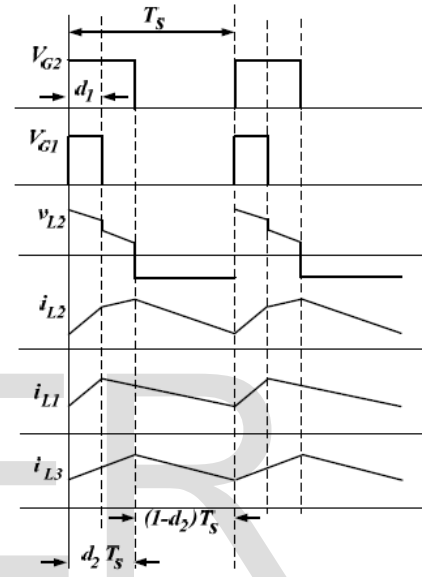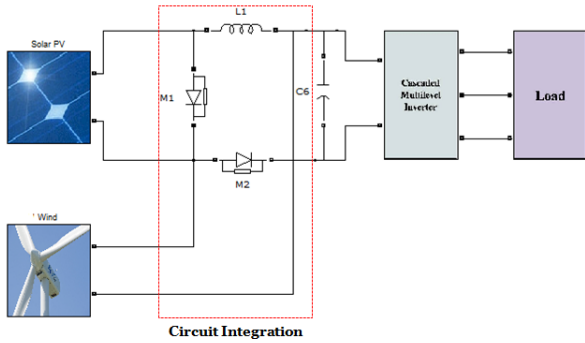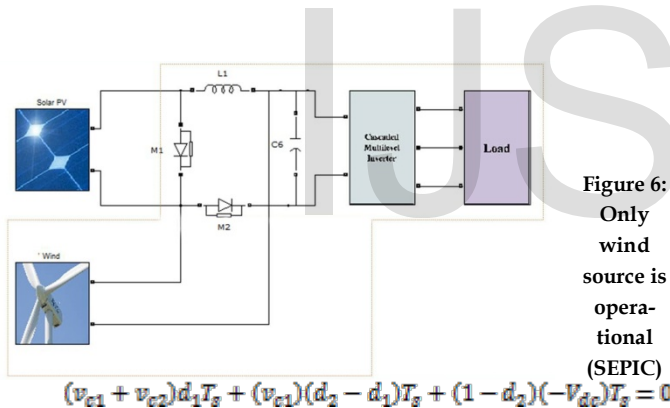**Figure 6: Only wind source is operational (SEPIC)**

$$(v_{c1} + v_{c2})d_1T_s + (v_{c1})(d_2 - d_1)T_s + (1 - d_2)(-V_{dc})T_s = 0$$

As for the current stress, it is observed from Figure 8 which is the peak current always occurs at the end of the on-time of the MOSFET.
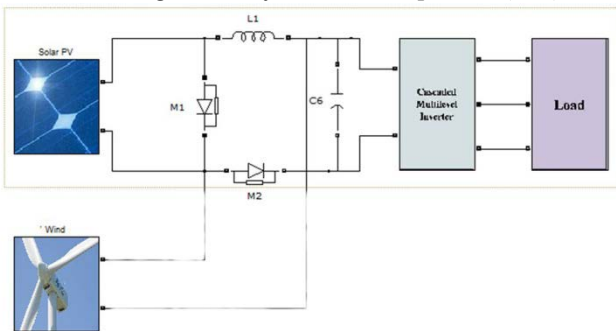
Figure 7: Only PV source is operation (Cuk)

The PV output current, which is also equal to the average input current of the Cuk converter, is given in (10). It can be observed that the average inductor current is a function of its

Fig8.

Proposed Circuit inductor Waveforms

$$L_{so1} = \frac{u_1 \cdot u_2}{r \cdot \cdot \cdot}$$
$$i_{ds2,pk} = I_{i,W} + I_{dc,avg} + \frac{w \cdot u_2 \cdot s}{2l}$$

$$L_{so2} = \frac{u_2 \cdot u_2}{r \cdot \cdot \cdot}$$

$$i_{i,pv} = \frac{r_o}{r} \cdot \frac{u_1}{\cdot} \qquad (10)$$

4 MPPT CONTROL OF PROPOSED CIRCUIT

A common inherent drawback of wind and PV systems is the intermittent nature of their energy sources.

The power coefficient (C_P) is a nonlinear function that represents the efficiency of the wind turbine to convert wind energy into mechanical energy. It is dependent on two variables, the tip speed ratio (TSR) and the pitch angle. The TSR, λ, refers to a ratio of the turbine angular speed over the wind speed.

Radius of turbine blade (r)
Wind velocity (Vw)
Blade Pitch angle (β)
Angular velocity (ωr)
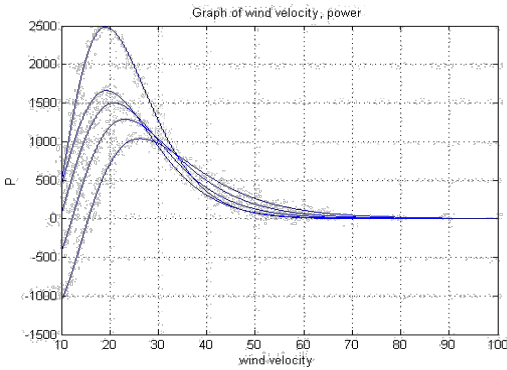Blade tip speed (λ) $\left(\lambda = \frac{r\omega_r}{v_w}\right)$
Turbine Power Coefficient (Cp)
Maximum value of Cp is 59.3% ≈ 0.59

$$c_p(\lambda,\beta) = c_1 \left[\frac{\pi z}{\lambda} - c_3\beta^x - c_4 \right] e^{\overline{\lambda_1}} + c_6\lambda$$

$$\frac{1}{\lambda} = \frac{1}{\lambda + 0.000} - \frac{0.000}{\beta^3 + 1}$$

x = different for various turbine design ,c1=0.5176,c2,116,c3=0.4,c4=5,c5=21,c6=0.0068

Figure 8:
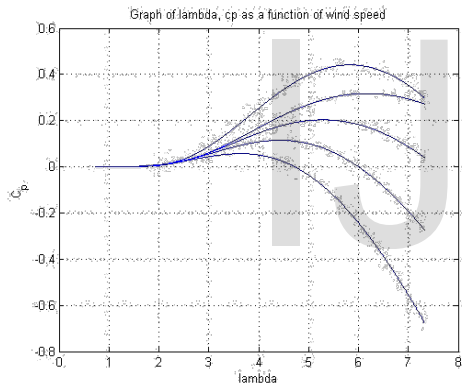**Power Coefficient Curve for a typical wind turbine**

Figure 9: Power Curves for a typical wind turbine

Hill climb search (HCS) a maximum power point tracking scheme allowed for shaping Solar and wind curves which is often applied to these energy sources to extract maximum power [16]. Conversely, if a negative change in the output power is observed, then the control algorithm will reverse the direction of the pervious perturbation step. In the case that the change in power is close to zero then the algorithm will invoke no changes to the system operating point since it corresponds to the maximum power point.The MPPT scheme employed in this paper is a version of the HCS strategy. Figure 10 is the flow chart that illustrates the implemented MPPT scheme.

In conventional multilevel inverters, the power semiconductor switches are combined to produce a high frequency waveform in positive and negative polarities. However, there is no need to utilize all the switches for generating bipolar levels.
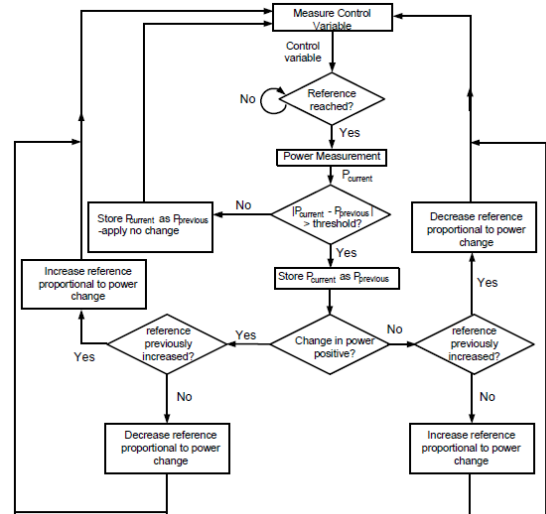

Figure 10: General MPPT Flow Chart for wind and PV

5 CASCADED MULTILEVEL INVERTER

The Cascade multilevel inverter subsists of a series of the H-bridge inverter units. The number of output phase voltage levels is 2S+1, where S is the number of DC sources and 's' is the number of H-bridges connected in cascade per phase. Among 's' number of switching angles, generally one switching angle is used for fundamental voltage selection and the remaining (s-1) switching angles are used to eliminate certain predominating lower order harmonics. In a three-phase system with isolated neutral, triplen harmonics are cancelled out automatically, and only non-triplen odd harmonics are present [17]. The fundamental voltage is obtained from the calculated switching angles α_1, α_2, α_3... α_n and 'n' represents the order of the harmonics and the switching angles are identical to the number of DC-sources. It is required to find the switching angles in the range of 0 to $\pi/2$ considering 3rd, 5th and 7th order phase voltage to zero.

The sum of all of the individual inverter outputs ($V_1+V_2+V_3=V_{out}$) is represented in Figure.5,is voltage waveform of series H-bridge inverter which are proficient by connecting the DC source to AC output by using multiple combinations of switches.

The Fourier series of the quarter-wave symmetric for the above staircase waveform is written as follows:

$$v_{out}(\omega t) = \sum_{n=1}^{\infty} \left[\frac{\pi v}{\pi} \sum_{k=1}^{S} \cos(n\alpha_k) \right] \sin(n\omega t) \qquad (11)$$

For seven level cascade inverter the fundamental voltage in terms of switching angles is given in equation (12).

$$V_1 = \frac{\pi v}{\pi} \sum_{k=1}^{S} \cos(\alpha_k) \qquad (12)$$

When all the switching angles are zero

Maximum fundamental voltage (V_{1max}) = $3 * \left(\frac{4V_{dc}}{\pi} \right)$

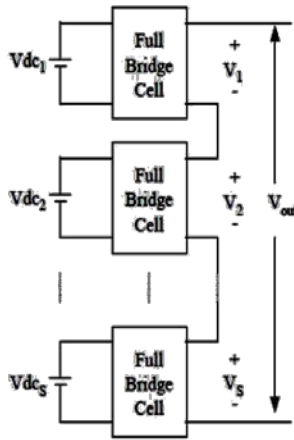Modulation index (M) = $\frac{V_1}{\frac{4V_{dc}}{\pi}}$ \qquad (13)

Fig.11: Schematic diagram of H-bridge series-connected multilevel inverter.
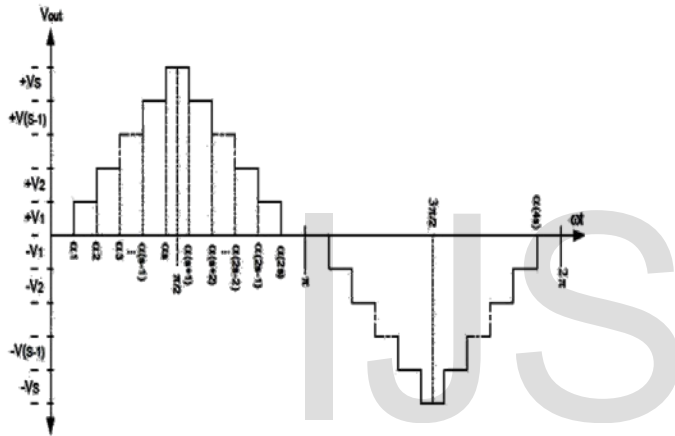

Fig.12: Switching angles of H-bridge series-connected multilevel inverter.

The general function of the cascade multilevel inverter is to incorporate a desired voltage from several separate DC sources as shown in Fig.4. Each DC Source is connected to an H-bridge inverter and can generate three different voltage outputs, +Vdc, 0 and –Vdc [18]. The sum of all of the individual inverter outputs ($V_1+V_2+V_3=V_{out}$) are represented in Figure.5,is voltage waveform of series H-bridge inverter which are proficient by connecting the DC source to AC output by using multiple combinations of switches. Cascade multilevel inverter generally incorporated with different voltage sources and in these proposed cascade multilevel inverter DC sources as shown in figure 6 are replaced by μgrid (Solar, wind and Fuel Cell)

The Fourier series of the quarter-wave symmetric for the above staircase waveform is written as follows:

$$v_{out}(\omega t) = \sum_{n=1}^{\infty} [\tfrac{4 v_{dc}}{n\pi} \sum_{k=1}^{S} \cos(n\alpha_k)] \sin(n\omega t) \qquad (14)$$

For seven level cascade inverter the fundamental voltage in terms of switching angles is given in equation (15).

$$V_1 = \tfrac{4 v_{dc}}{\pi} \sum_{k=1}^{S} \cos(\alpha_k) \qquad (15)$$

When all the switching angles are zero

Maximum fundamental voltage (V_{1max}) $= 3 * (\tfrac{4 V_{dc}}{\pi})$

Modulation index (M) $= \dfrac{V_1}{\tfrac{4 V_{dc}}{\pi}}$ $\qquad$ (16)

The 7-level cascaded inverter requires three H-bridges. The non linear equations which are used to finding the switching angles and desired fundamental voltage of 7-level inverter are equations (17), (18), (19) and (20).

$$[\cos(\alpha_1) + \cos(\alpha_2) + \cdots + \cos(\alpha_s)] = \tfrac{S M \pi}{4} \qquad (17)$$

$$[\cos(3\alpha_1) + \cos(3\alpha_2) + \cdots + \cos(3\alpha_s)] = 0 \qquad (18)$$

$$[\cos(5\alpha_1) + \cos(5\alpha_2) + \cdots + \cos(5\alpha_s)] = 0 \qquad (19)$$

$$[\cos(7\alpha_1) + \cos(7\alpha_2) + \cdots + \cos(7\alpha_s)] = 0 \qquad (20)$$

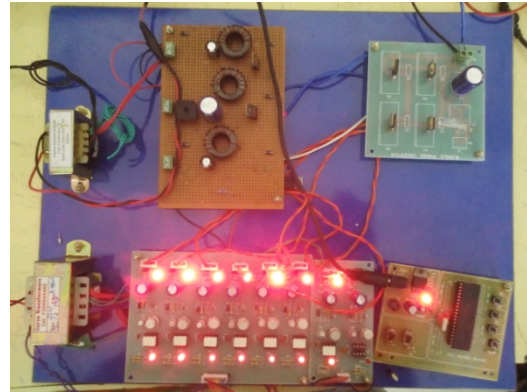## 6 HARDWARE AND SIMULATION RESULTS

Fig.13:
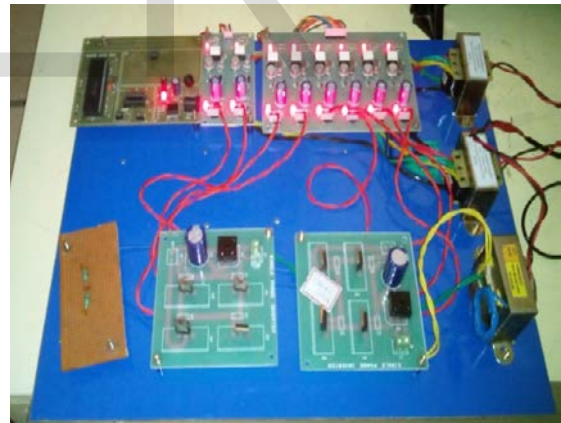**Design of Hardware Rectifier Stage Topology with 3-levelinverter**

Fig.14
: Design of Hardware Rectifier Stage Topology with 5-levelinverter

Table 2: Switching Values of different Iterations using NR Method

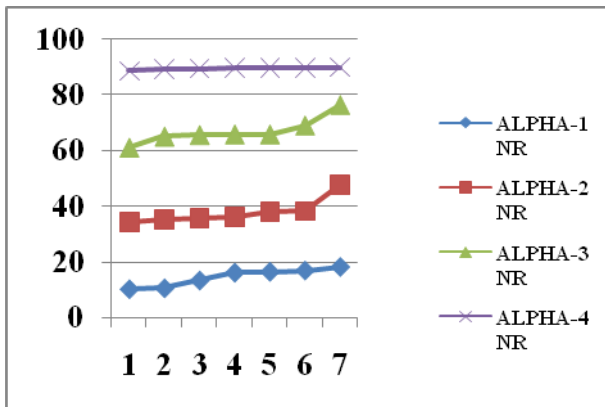| NR Method					
	α1	α2	α3	α4	THD%
ITR1	18.113	47.755	76.420	89.9	16.47%
ITR2	10.536	35.286	65.172	89.358	16.18%
ITR3	10.222	34.287	61.170	88.682	15.70%
ITR4	13.291	35.605	65.702	89.499	15.19%
ITR5	16.818	38.241	69.090	89.8	14.27%
ITR6	16.414	38.147	65.921	89.785	13.54%
ITR7	16.102	36.213	65.919	89.710	13.27%

Fig.15: Graphical representation of different Switching Values

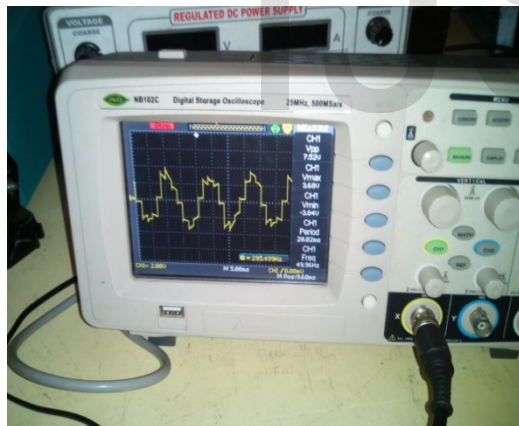**Fig.16: Output Waveform of three level cascaded Inverter**

Fig 17: Output Waveform of five level Inverter

7 CONCLUSION

Now-a-days, The Microgrid is aggregations of resources are-connected to the different application as DC source. In this paper, an alternative multi-input rectifier topology is proposed for μ-grid (hybrid Solar/Wind system). Hardware de-

sign is a blend of the Cuk and SEPIC converters. The proposed topology will give a scope for the use of μ-grid with MPPT for individual source and rectification circuits. Hardware and Simulation results are lend to check with the utility of the proposed system

REFERENCES

[1] Y. Ito, Z. Yang, and H. Akagi, "DC Microgrid Based Distribution Power Generation System," in Proc. IEEE Int. Power Electron. Motion Control Conf., vol. 3, pp. 1740-1745, Aug. 2004

[2] P. Chiredeja and R. Ramakumar, "An approach to quantify the technical benefits of distributed generation," IEEE Trans. Energy Conversation, vol.19, no. 4, pp. 746-773, Dec. 2004.

[3] T.E. McDermott and R.C. Dugan, "Distributed Generation Impact on Reliability and Power Quality" in Proc. of IEEE Conf. on Rural Electric Power,2002, pp. D3-D3_7.

[4] S.K. Kim, J.H Jeon, C.H. Cho, J.B. Ahn, and S.H. Kwon, "Dynamic Modelling and Control of a Grid-Connected Hybrid Generation System with Versatile Power Transfer," IEEE Transactions on IndustrialElectronics, vol. 55, pp. 1677-1688, April 2008.

[5] Arulampalam, N. Mithulananthan, R.C. Bansal, and T.K. Saba, "Micro grid Control of PV -Wind-Diesel Hybrid System with Islanded and Grid Connected Operations," in Proc. IEEE Int. Conf. Sustainable Energy Technologies, pp. 1-5, 2010

[6] N. A. Ahmed, M. Miyatake, and A. K. Al-Othman, "Power fluctuations suppression of stand-alone hybrid generation combining solar photovoltaic/wind turbine and fuel cell systems," in Proc. Of EnergyConversion and Management, Vol. 49, pp. 2711-2719, October 2008

[7] S. Jain, and V. Agarwal, "An Integrated Hybrid Power Supply for Distributed Generation Applications Fed by Nonconventional Energy Sources," IEEE Transactions on Energy Conversion, vol. 23, June2008

[8] S.L. Helter et.al, "photovoltaic module and array evaluation,"IEEE 1984,pp 700-704.

[9] T.Ackermann, wind power in power systems, wileyNew York, 2005.

[10] R. W. Erickson, "Some Topologies of High Quality Rectifiers" in theProc. of the First International Conference on Energy, Power, and Motion Control, May 1997.

[11] D. S. L. Simonetti, J. Sebasti´an, and J. Uceda, "The DiscontinuousConduction Mode Sepic and ´Cuk Power Factor Preregulators: Analysis and Design" IEEE Trans. On Industrial Electronics, vol. 44,no. 5, 1997

[12] N. Mohan, T. Undeland, and W Robbins, "Power Electronics: Converters, Applications, and Design," John Wiley & Sons, Inc., 2003.

[13] J. Marques, H. Pinheiro, H. Grundling, J. Pinheiro, and H. Hey, "A Survey on Variable-Speed Wind Turbine System," Proceedings of Brazilian Conference of Electronics of Power, vol. 1, pp. 732-738,2003.

[14] F. Lassier and T. G. Ang, "Photovoltaic Engineering Handbook" 1990

[15] Global Wind Energy Council (GWEC), "Global wind 2008report,"June 2009.

[16] L. Pang, H. Wang, Y. Li, J. Wang, and Z. Wang, "Analysis of Photovoltaic Charging System Based on MPPT," Proceedings of Pacific-Asia Workshop on Computational Intelligence and Industrial Application 2008 (PACIIA '08), Dec 2008, pp. 498-501.

[17] John N. Chiasson, Leon M. Tolbert, "Elimination of Harmonics In Multilevel Inverters Using the theory of Symmetric polynomial and Resultant" Proceedings of the 42nd IEEE Conference on Decision and Control Maui, Hawaii USA, December 2003.

[18] Zhong Du, Leon M. Tolbert, John N. Chiasson "Reduced Switching Frequency Computed PWM method for multilevel converter control" Power Electronics Specialists Conference, 2005. PESC '05. IEEE, 2005, Page(s): 2560 – 2564.

_____

• *M.Manigandan is currently working as Assistant Professor in Department of EEE at GITAM University, Hyderabad. E-mail:manimatlab@gmail.com*
• *Dr.B.Basavaraja is currently working as Professor & Chairman at University BDT College of Engineering.E-mail: banakara36@gmail.com*
• *G.Srikanth currently pursuing Masters in Power systems and Automation at GITAM University Hyderbad .Email:srikanthg345@gmail.com*